Development 118, 105-115 (1993)
Printed in Great Britain © The Company of Biologists Limited 1993

Control of imaginal cell development by the *escargot* gene of *Drosophila*

Shigeo Hayashi[1], Susumu Hirose[1], Tony Metcalfe[2] and Alan D. Shirras[2,*]

[1]DNA Research Center, National Institute of Genetics, Mishima, Shizuoka-ken 411, Japan
[2]Division of Biological Sciences, Institute of Environmental and Biological Sciences, Lancaster University, Lancaster LA1 4YQ, UK

*Author for correspondence

SUMMARY

Mutations in the *escargot* (*esg*) locus, which codes for a zinc-finger-containing protein with similarity to the product of the *snail* gene, cause a variety of defects in adult structures such as loss of abdominal cuticle and malformation of the wings and legs. *esg* RNA is expressed in wing, haltere, leg and genital imaginal discs and in abdominal histoblast nests in the embryo. Expression in imaginal tissues is also found in third instar larvae. In *esg* mutant larvae, normally diploid abdominal histoblasts replicate their DNA without cell division and become similar in appearance to the polytene larval epidermal cells. A similar phenotype was also found in imaginal discs of larvae mutant for both *esg* and the *Drosophila raf* gene. These results suggest that one of the normal functions of *esg* may be the maintenance of diploidy in imaginal cells.

Key words: *Drosophila*, histoblast, imaginal disc, ploidy, *escargot* gene

INTRODUCTION

During metamorphosis, holometabolous insects such as *Drosophila* undergo dramatic changes in external and internal morphology. Many of the larval cells disintegrate and adult body parts are constructed from groups of imaginal cells which originate during embryogenesis and are set aside from cells destined to form the larva. In Diptera, the larval epidermal cells, in common with a number of other larval cell types, become hypertrophied and polytene during larval stages (Pearson, 1974). In contrast, imaginal cells remain small and diploid during larval development. The cuticular structures of the adult head, thorax and genitalia are derived from the imaginal discs which undergo cell division in the larva and then evert to produce adult structures during metamorphosis. The epidermis of the adult abdomen is derived from groups of imaginal cells known as the histoblast nests. These cells are contiguous with the larval epidermis and synthesize larval cuticle (Madhavan and Schneiderman, 1977). Unlike the imaginal disc cells, they do not divide during larval development but begin to divide rapidly approximately 3 hours after pupariation, doubling every 3.6 hours. Then, at approximately 15 hours after pupariation, the cells begin to migrate, displacing the larval epidermal cells which are histolysed (Roseland and Schneiderman, 1979). There are four pairs of histoblast nests per segment: two dorsal pairs, one anterior and one posterior which give rise to the tergite, a ventral pair which gives rise to the sternite and the pleura and a spiracular pair which gives rise to the perispiracular epidermis (Roseland and Schneiderman, 1979). The anterior dorsal nests contain 12-14 cells, the posterior dorsal nests 6-7 cells and the ventral nests 12-13 cells (Madhavan and Schneiderman, 1977).

Mutations at the *l(2)35Ce* locus cause embryonic or early larval lethality but rare escapers have poorly differentiated adult abdomens (Ashburner et al., 1990). This locus has recently been cloned and termed *escargot* (*esg*; Whiteley et al., 1992). *esg* codes for a zinc finger protein with similarity to the product of the *snail* gene. In this study we describe the expression of *esg* in imaginal tissues and the mutant phenotype of *esg* allelic combinations that survive to the pharate adult or adult stage. Our analyses of abdominal histoblasts and imaginal discs in *esg* mutant larvae suggest that one of the functions of *esg* is to maintain diploidy of imaginal cells by suppressing the endoreplication which occurs in larval cells.

MATERIALS AND METHODS

Stocks

esg^{P1} was isolated from a second chromosome P-element mutagenesis. P-elements were mobilized from the Q strain Athens 77 (J. Merriam, personal communication) by crossing to the stable transposase-producing strain delta 2-3 (99B) (Robertson et al., 1988). Mutagenised chromosomes were balanced over *CyO*. The enhancer trap line esg^{P2} was isolated using methods and stocks described by Bier et al. (1989). To induce lethal mutations flanking the esg^{P2} insert, the P element was mobilized from the isogenised esg^{P2} chromosome by P-element transposase supplied from the delta 2-3(99B) strain. The lethal enhancer trap line esg^{P3} was isolated from the collection of P-element lethal mutations held in the laboratory of Allen Spradling at the Carnegie Institution of

Washington, Baltimore (originally designated *l(2)5729*) and kindly provided by Michael Ashburner and John Roote. The EMS-induced *esg* alleles VS2 and VS8 were isolated previously (Ashburner et al., 1990). These and deficiencies with breakpoints in the *esg* region were provided by Michael Ashburner and John Roote. *Df(2L)A48* uncovers the entire *esg* gene. *CyO,ftzlacZ* made by Yash Hiromi was obtained from Chris Doe. The *y raf*^{1} stock was obtained from Yasuyoshi Nishida. All other stocks are described in Lindsley and Zimm (1992).

In situ hybridisation

In situ hybridisation of embryo whole mounts using digoxigenin (DIG)-labelled probes (Boehringer Mannheim) was carried out essentially as described by Tautz and Pfeifle (1989) with the following modifications. Initial fixation was in 50 mM EGTA and 10% paraformaldehyde in PBS. After methanol devitellinisation, embryos were stored in methanol at –20°C. Embryos were treated with 0.3% H_2O_2 in methanol for 20 minutes at room temperature and rinsed twice with methanol, once with a 1:1 mixture of methanol and 5% paraformaldehyde in PBTw (Tautz and Pfeifle, 1989) for 5 minutes and then postfixed in 5% paraformaldehyde in PBTw for 20 minutes. Proteinase K digestion and hybridisation were carried out as described. Hybridised embryos were washed once in hybridisation buffer, once in a 1:1 mixture of hybridisation buffer and PBTw for 20 minutes at 48°C, and 5× 5 minutes in PBTw at room temperature. Incubation with preabsorbed anti-DIG antibody and detection were as described. Stained embryos were mounted in 80% glycerol or dehydrated in ethanol, rinsed with xylene and mounted in DPX (Fluka). Probe DNA was labelled using a Genius kit (Boehringer Mannheim) with modifications suggested by Ephrussi et al. (1991). To detect *esg* expression, genomic DNA containing the entire *esg* transcription unit or cDNA (S. Hayashi, unpublished) was used as a probe. Imaginal discs were prepared and hybridised as described by Kramer and Zipursky (1990).

Localisation of β-galactosidase

X-gal staining of third instar larvae was carried out as described (method 77 in Ashburner, 1989).

To study the *esg*^{P3}*/Df(2L)A48* embryonic phenotype, embryos from a cross between mutant stocks balanced over *CyO,ftz-lacZ* (Df was supplied from male) were collected, dechorionated, fixed in a 1:1 mixture of heptane and 4% formaldehyde in PBS, methanol devitellinised, and treated with 0.3% H_2O_2 in methanol for 20 minutes. Embryos were rehydrated and blocked in TBST (10 mM Tris-HCl pH 7.5, 130 mM NaCl, 1 mM EDTA, 0.1% BSA, 0.1% Triton X-100) for 1 hour and then incubated with a mixture of mouse monoclonal antibodies against β-galactosidase (Promega, 1:1000 dilution). The embryos were washed 5 times for 10 minutes and incubated with biotin-conjugated sheep anti-mouse IgG (Amersham) for at least 1 hour. After washing, the embryos were incubated in a 1:200 dilution of ABC complex (ABC elite kit, Vector Labs) for at least 30 minutes and washed again. Staining was developed in 50 mM Tris-HCl pH 7.5, 0.5 mg/ml diaminobenzidine (DAB), 0.04% NiCl and 0.01% H_2O_2. The embryos were dehydrated, mounted in methyl salicylate and observed under Nomarski optics. *esg* mutant embryos were identified by the absence of *ftz-lacZ* expression.

Immunofluorescent analysis of larval tissues

The *esg*^{P3}*/esg*^{V8} larval mutant phenotype was examined in the progeny of crosses between *esg*^{VS8}*/Bc* males and *esg*^{P3}*/CyO* or *y raf*^{1}*/Binsc;esg*^{P3}*/CyO*. The larval tissues were immunostained as described (Tomlinson and Ready, 1987) using rabbit anti-β-galactosidase (Cappel, 1:250 dilution) and FITC-conjugated anti-rabbit IgG (Vector Labs, 1:100 dilution) and then counterstained with 0.5 μg/ml of propidium iodide (PID) in PBS, mounted in 80% glycerol in 100 mM Tris-HCl, pH 8.8 and 2.5% 1,4-diazabicyclo-[2.2.2]octane and observed with a fluorescence microscope or Zeiss laserscan confocal microscope. The genotype of larvae was identified by β-galactosidase staining and the *y* and *Bc* (*Black cell*) markers.

Quantification of DAPI fluorescence

OregonR wild-type or *esg*^{P3}*/esg*^{VS8} wandering third instar larvae (identified as *Tb*$^{+}$ progeny from a cross between *esg*^{P3}*/SM5-TM6B,Tb* and *esg*^{VS8}*/SM5-TM6B,Tb*) were bisected longitudinally along the dorsal midline with a sharp razor blade, the gut and fat body were removed and the body walls fixed in 90% ethanol, 5% acetic acid for 10 minutes. The musculature was removed prior to rinsing with phosphate-buffered saline (PBS; 3× 3 minutes) and with 180 mM Tris-HCl, pH 7.5 (1× 3 minutes). The body walls were stained with 0.5 μg/ml DAPI (4,6-diamidino-2-phenylindole) in 180 mM Tris-HCl, pH 7.5 for 15 minutes, washed with PBS and mounted in 80% glycerol. Relative fluorescence was measured on a Nikon Diaphot inverted epifluorescence microscope linked to a Cairn spectrophotometer system (Cairn Research Ltd. Kent, UK). A rectangular diaphragm and a ×40 oil immersion objective were used to restrict measurements to single nuclei. The position of histoblasts was determined relative to insertion sites of transverse muscles.

BrdU labelling of larval tissues

Endoreplication of DNA was determined using an immunocytochemical cell proliferation kit (Amersham). Larvae were transferred as early second instars (48 hours after egg laying) to food containing 30 μl of labelling reagent in 3 ml of medium (5-bromo-2′bromodeoxyuridine, 30 μg/ml and 5-fluoro-2′-deoxyuridine, 3 μg/ml final concentrations). Larvae were allowed to develop to the wandering third instar stage at 25°C. They were then bisected and fixed in acid ethanol as described above. Endogenous peroxidase activity was reduced by incubation in 2% H_2O_2 in methanol for 10 minutes. The body walls were then rehydrated in PBS (3× 3 minutes) and incubated in 0.5% BSA, 0.3% Triton X-100 in PBS for 1 hour at room temperature. Anti-BrdU monoclonal antibody/nuclease was diluted according to the manufacturer's instructions and the body walls incubated with 100 μl of the diluted mixture at 4°C for 16 hours with constant mixing. The body walls were washed in PBS, 0.3% Triton X-100 (PBST) for 6× 30 minutes and then incubated in 50% normal goat serum in PBS at room temperature for 1 hour. Peroxidase-conjugated anti-mouse second antibody was diluted according to the manufacturer's instructions and the specimens incubated with 100 μl of the diluted antibody for 2 hours at room temperature with constant mixing. The body walls were washed in PBST (5× 30 minutes) then in PBS (1× 30 minutes) and developed with DAB/H_2O_2 according to the manufacturer's instructions. The colour reaction was stopped by rinsing with PBS and the specimens were dehydrated, cleared in Histoclear (National Diagnostics) and mounted in Histomount (National Diagnostics).

In vitro labelling of epidermis from pre-pupae with BrdU was carried out by bisecting puparia 5 hours after puparium formation, removing the gut and flushing out the larval fat body before incubating in a 1:500 dilution of labelling reagent in Ringer's solution for 1 hour at room temperature. Fixation and antibody detection steps were as described above.

Haematoxylin staining

Puparia were bisected, cleaned and fixed in acid-ethanol as described above. Puparia with attached epidermis, or pupal cuticle plus epidermis, were transferred to Hansen's haematoxylin (Solcia, 1973) for 15 minutes and then rinsed repeatedly with tap

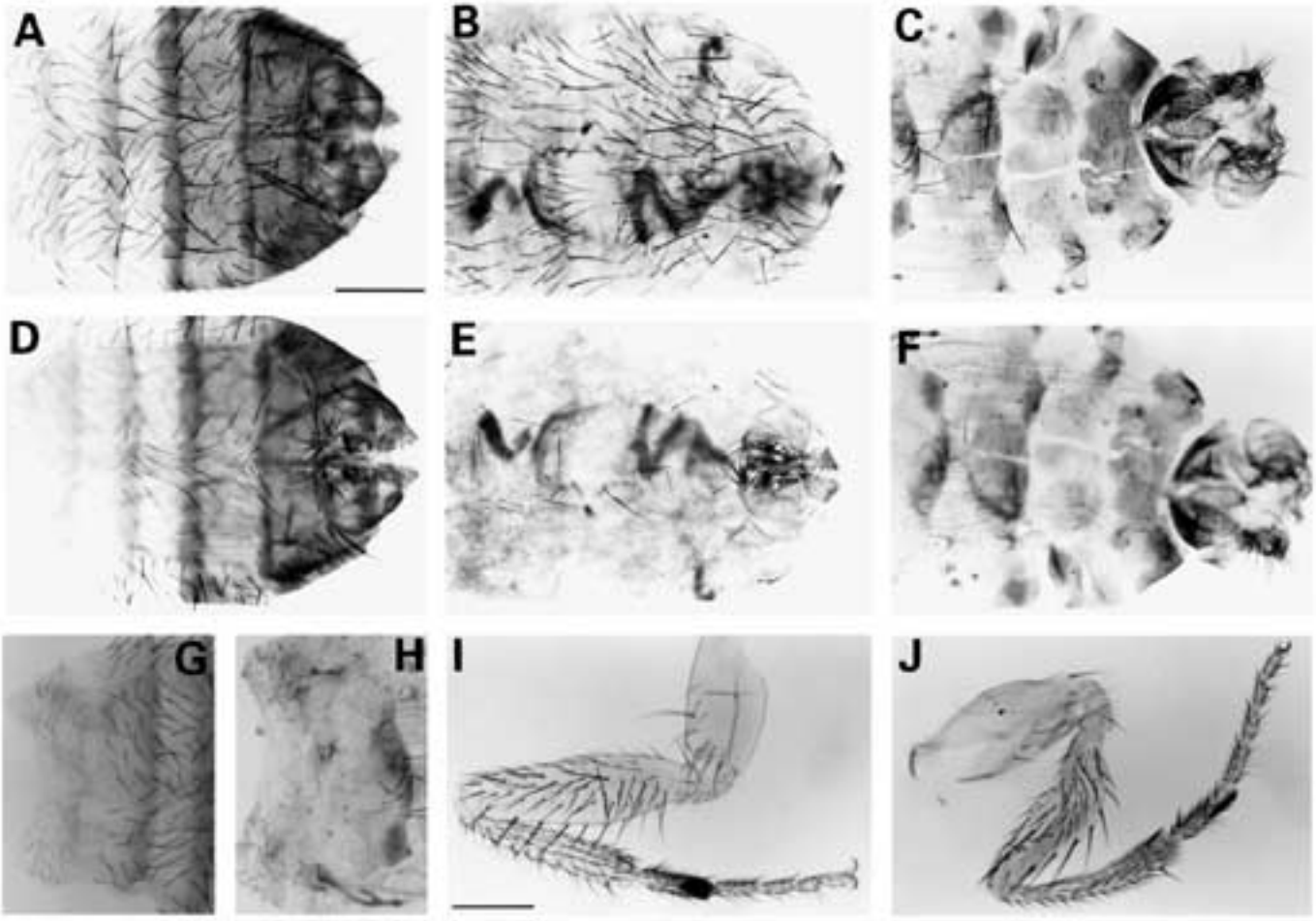

Fig. 1. Examples of defects in adult cuticular structures caused by *esg* mutations. (A, D) OregonR male abdomen. (A) Dorsal view. (D) Ventral view. (B, E) Abdomen of an esg^{P1} homozygous male, an example of the mild abdominal phenotype. (B) Dorsal view. The tergites are relatively unaffected with only occasional missing, or misaligned, bristles. (E) Ventral view. The sternites are partially deleted. (C, F) Abdomen of an esg^{VS8}/esg^{GW2} male, an example of the severe abdominal phenotype. (C) Dorsal view. The tergites are almost completely deleted. (F) Ventral view. The sternites are completely deleted. (G) Dorsal view of a male OregonR abdomen showing segments A1-A3. (H) Dorsal view of an esg^{VS8}/esg^{GW2} male abdomen showing segments A1-A3. A1 is relatively unaffected and retains most of the microchaetae. (I) OregonR male prothoracic leg. (J) esg^{VS8}/esg^{L6} male prothoracic leg. Note the twisted femur. Scale bar in A, 2005 μm; in I, 1005 μm.

water for 30 minutes. The specimens were dehydrated, cleared in Histoclear (National Diagnostics) and mounted in Histomount (National Diagnostics).

RESULTS

Viability and phenotype of *esg* alleles

Table 1 lists the viability and phenotype of combinations of different *esg* alleles and combinations of alleles and deficiencies. The EMS-induced alleles esg^{VS2} and esg^{VS8} have been previously described (Ashburner et al., 1990). The esg^{P1} allele and the lethal enhancer trap allele, esg^{P3}, were caused by insertions close to the transcription start site (S. Hayashi, unpublished observations). Additional alleles (L2, L3, L6 and L7) were isolated by P-element excision from the viable enhancer trap line esg^{P2}. The esg^{L2} allele has lost part of the *esg* transcription unit (S. Hayashi, unpublished observations) and is probably equivalent to the 'null' esg^{G66} allele reported by Whiteley et al. (1992). In addition, several deficiencies that have one of their breakpoints near the *esg* locus behave as *esg* hypomorphs when combined with *esg* alleles. Such deficiencies are *Df(2L)TE116(R)GW2*, *Df(2L)TE116(R)GW21*, and *Df(2L)TE116(R)GW13* (Ashburner et al., 1990) and we will refer to them as esg^{GW2}, esg^{GW21} and esg^{GW13}.

As can be seen from Table 1, flies that die as pharate adults generally have defects of varying severity in the adult abdomen, the exception being crosses involving esg^{L7}. esg^{P1} homozygotes have a mild abdominal phenotype with some missing or misaligned bristles on the tergites and sternites (Fig. 1B,E). All alleles in combination with the deficiency esg^{GW2} are viable or semi-viable with defects in the abdomen, the severity of which is allele-dependent. Most severe is the esg^{GW2}/esg^{VS8} combination (Fig. 1C,F). These flies completely lack sternites but have some bristles and patches of pigment on the dorsal surface of the abdomen. The regular rows of bristles found on the pleura of wild-

type flies are disrupted. The first abdominal segment of flies with severe abdominal defects is much less affected than the rest of the abdomen. Fig. 1H shows the anterior segments of the abdominal cuticle of esg^{GW2}/esg^{VS8}. Comparison with the same region of cuticle from a wild-type fly shows that most of the microchaetae are present in the first abdominal segment while most bristles are missing from the second and third abdominal segments. The external genitalia of all allelic combinations are normal and viable allelic combinations are fertile.

Some allelic combinations show defects in structures derived from imaginal discs, for example many of the viable combinations show a held-out wing phenotype and most allelic combinations which die at the pharate adult stage have twisted legs (Fig. 1J). Rare esg^{P1}/esg^{GW21} pharate adults have a reduced eye and an abnormal maxillary palp (data not shown). Since the defects in abdomen, held out wing and twisted legs are seen in several different allelic combinations, it is likely that these phenotypes are the result of partial loss of *esg* function.

esg expression during embryogenesis

The expression of the *esg* gene in late embryogenesis was studied by whole-mount in situ hybridisation. At stage 14, several clusters of cells, which are likely to correspond to the wing, haltere, leg and genital imaginal discs and the abdominal histoblast nests, start to express *esg* RNA (Fig. 2A,B). In A1-A7, there were seven sets of putative abdominal histoblasts embedded in the epidermis (Fig. 2C,D). The central part of the leg disc does not express *esg* RNA (Fig. 2A). This part will probably give rise to Keilin's organ. Therefore, *esg* expression is imaginal-cell-specific in the case of the leg disc. In addition to the expression in imaginal cells, *esg* RNA was also detected in the central nervous system, tracheae and head of stage-14 embryos (Fig. 2A). The central nervous system and tracheal expression decays during later stages, though the head expression persists until late in embryogenesis. These results are, in general, consistent with the findings of Whiteley et al. (1992).

To examine the possible role of *esg* in formation of the imaginal discs and histoblasts, the expression of β-galactosidase from the enhancer trap esg^{P3} was examined in a *Df(2L)A48* background. esg^{P3} is a strong allele and larvae with this genotype die before pupation. esg^{P3} expresses *lacZ* in imaginal discs and in abdominal histoblasts in a pattern identical to *esg* RNA expression. The anti-β-galactosidase staining pattern of $esg^{P3}/Df(2L)A48$ embryos was the same as control $esg^{P3}/CyO\text{-}ftzlacZ$ embryos. Loss of *esg* activity, therefore, does not cause any apparent defects in the formation of imaginal tissues as judged by the pattern of *lacZ* expression from the esg^{P3} enhancer trap element.

esg expression in third instar larvae

Expression of *esg* in imaginal tissues in third instar larvae was investigated by in situ hybridisation. *esg* RNA was detected in several imaginal discs and in the central nervous system. Examples of imaginal disc expression are

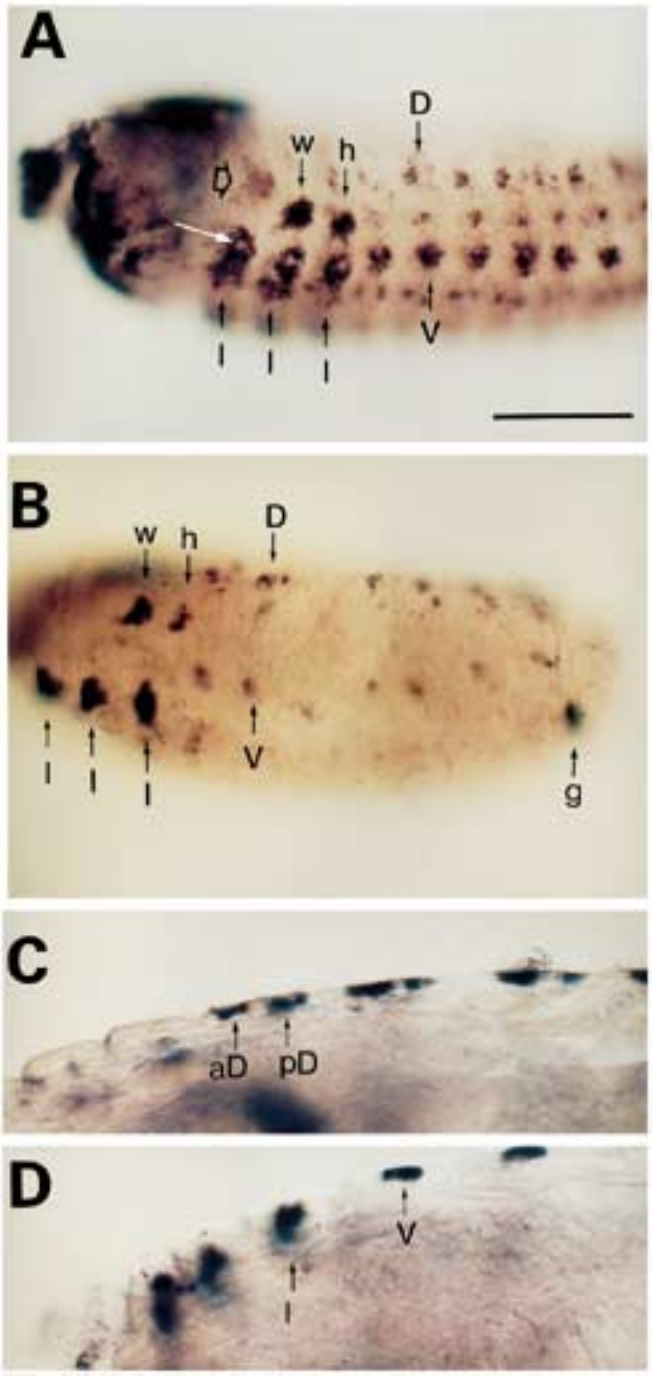

Fig. 2. *esg* RNA expression in embryonic imaginal tissues detected by whole-mount in situ hybridisation. Unless indicated, all embryos are oriented with anterior to the left and dorsal uppermost. (A) Stage-14 embryo. *esg* RNA is first detected in imaginal cell primordia at this stage. w, wing disc; h, haltere disc; l, leg disc; D, dorsal A2 abdominal histoblast nest and V, ventral A2 abdominal histoblast nest. A white arrow indicates cells lacking *esg* expression which will probably become Keilin's organ. An arrowhead indicates the anterior spiracle. (B) Stage-16 embryo. *esg* RNA is restricted to imaginal cells and the head. g, genital disc. (C) Horizontal optical section of a stage-16 embryo showing anterior dorsal (aD) and posterior dorsal (pD) abdominal histoblast nests. (D) Different focal plane of the same embryo as in C. Ventral abdominal histoblasts (V) and leg disc (l) are indicated. Note that the histoblasts are embedded in the epidermis but the leg disc has invaginated. Scale bar in A, 10 μm. A and B are the same magnification; C and D are 2× larger.

Table 1. Complementation of various *esg* alleles

	DfA48	L2	L6	P3	VS2	VS8	P1	L7
L2	L	L						
L6	L	L	L					
P3	L	L	L	L				
VS2	L	PA S|N	PA I~S|S	PA S|?	L			
VS8	L	PA S|N	PA I~S|N	PA S|?	L	L		
P1	L	PA M~I|N	PA M|N	PA I|?	PA M~I|N	PA M|S	PA M|N	
L7	PA N|S	PA N|N	PA N|M	V†* N|N	V* N|M	V N|M	V†* N|M	V† N|N
GW21		L	L	L	L	L	L**	PA N|S
GW2		V† M|N	V† M~I|?	V† I|N	semiV† I~S|M	semiV† S|M	V† M|N	V N|N
GW13		V† N|N		V† M|N	V† M|M	V† M|N	V N|N	V N|N

In the upper row of each genotype, the lethal phase is indicated. Lethal phases were determined by counting flies with the relevant genotype and unhatched pupae. L, larval or embryonic lethal. No dead pupae observed. PA, pharate adult lethal. V, viable.

In the lower row, defects in abdomen (left) and leg (right) of mutant adults or pharate adults are indicated. Abdominal phenotype: N, normal; M, mild. Sternites are partially deleted. Tergites have a small number of missing or misaligned bristles and unpigmented patches, particularly at the lateral edge. I, intermediate. Sternites are completely deleted. Tergites are partially deleted. S, severe. More than half of the tergites are deleted. Leg phenotype: M, mild. Legs are slightly bent. S, severe. Legs are twisted at femur. Only found in lethal pupae.

†Held-out wing.

*Sick. Die within three days.

**Very few animals survive to the pharate adult stage with severe defects in the head, a reduced eye and mild defects in the abdomen. Twisted legs.

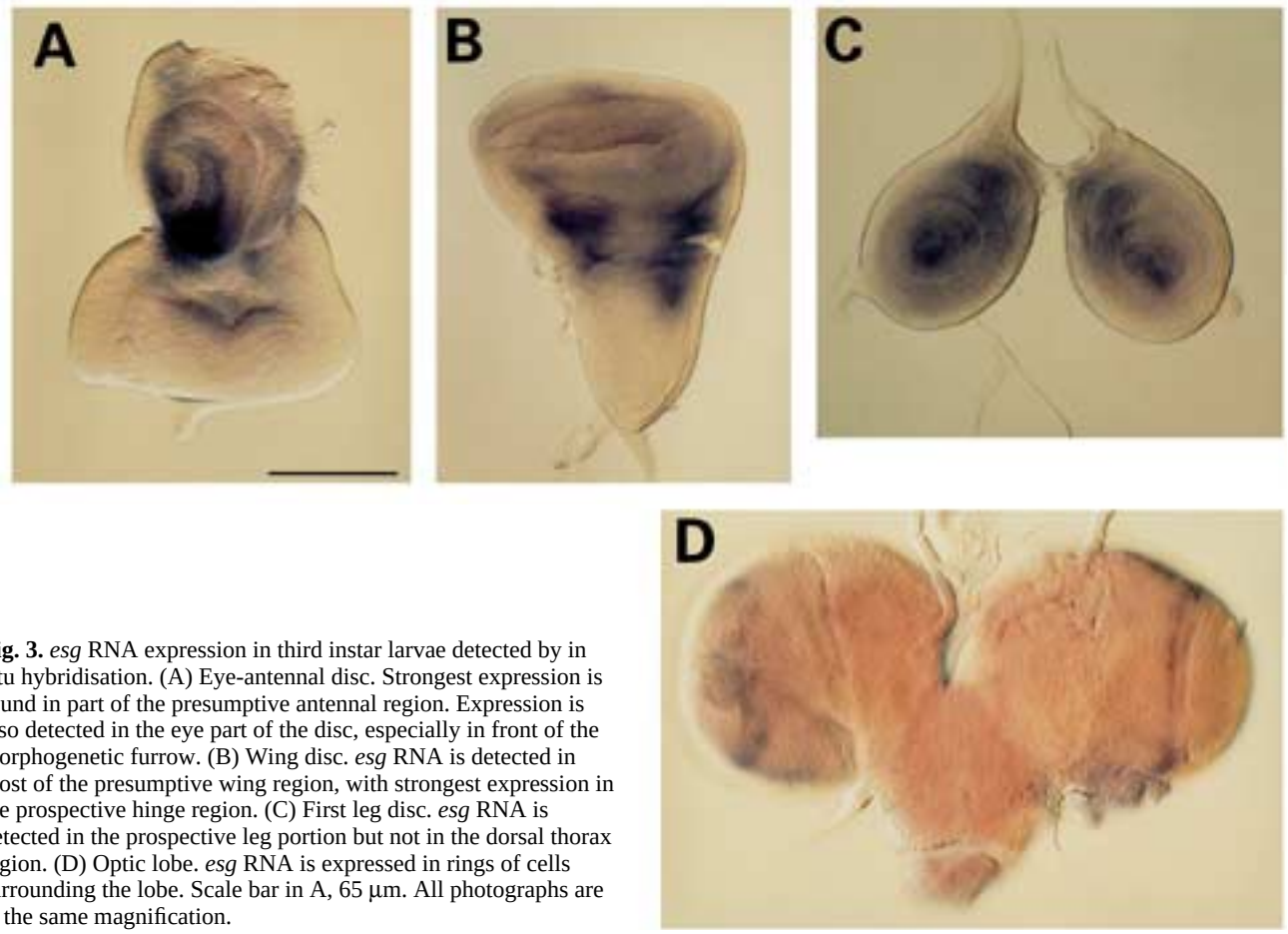

Fig. 3. *esg* RNA expression in third instar larvae detected by in situ hybridisation. (A) Eye-antennal disc. Strongest expression is found in part of the presumptive antennal region. Expression is also detected in the eye part of the disc, especially in front of the morphogenetic furrow. (B) Wing disc. *esg* RNA is detected in most of the presumptive wing region, with strongest expression in the prospective hinge region. (C) First leg disc. *esg* RNA is detected in the prospective leg portion but not in the dorsal thorax region. (D) Optic lobe. *esg* RNA is expressed in rings of cells surrounding the lobe. Scale bar in A, 65 μm. All photographs are at the same magnification.

shown in Fig. 3A-C. In the eye-antennal disc, *esg* RNA is expressed in most of the antennal part with especially strong expression in the prospective antennal region. *esg* RNA is also detected around the morphogenetic furrow. In the wing disc, *esg* RNA expression is restricted to the prospective wing region, especially in the hinge region. In the first leg disc, the expression is restricted to the central part of the disc, which will give rise to the leg. In each of these three examples, *esg* RNA is expressed most strongly in the distal part of the discs, which will give rise to appendages (Bryant, 1978), but not in the proximal part of the discs. A similar pattern of expression was detected in the other two leg discs and in the haltere disc. *esg* RNA was detected in a region of the optic lobe of the brain (Fig. 3D) which probably corresponds to the outer proliferation zone where imaginal neuroblasts are dividing. In addition, we found that the enhancer trap esg^{P3} expresses *lacZ* in most of the imaginal tissues of the third instar larva (data not shown).

Phenotype of *esg* mutant histoblasts

The enhancer trap line esg^{P3} expresses *lacZ* in abdominal histoblasts in embryos and third instar larvae. Animals with the genotype esg^{P3}/esg^{VS8} die as pharate adults with almost complete deletion of tergites and sternites (Fig. 4D,H). Abdominal histoblasts were examined in these mutants at the third instar larval stage using *lacZ* expression as a marker for the histoblasts. Mutant histoblasts expressed *lacZ* at higher levels than in controls (Fig. 4A,E) while the number of histoblasts per nest remains the same (Table 2). A similar phenotype was also observed in esg^{P3}/esg^{VS2} and esg^{P3}/esg^{GW2} larvae. In each case, the nuclei of the mutant histoblasts were larger than the controls (Table 2). Histoblasts of esg^{P3}/esg^{VS8} larvae were further analysed by staining with anti-β-galactosidase antibodies and the DNA binding dye propidium iodide (PID). In control larvae, abdominal histoblast nuclei were smaller and their PID staining was weaker than the surrounding larval epidermal cell nuclei. In *esg* mutant larvae, lacZ-positive cells were much larger and the intensity of PID staining was stronger and more uniform, resembling the larval epidermal cells (Fig. 4F,G). The diameter of the nuclei of mutant histoblasts is about 1.5-fold larger than the controls, which translates into a 3.4-fold increase in nuclear volume (Table 2).

Quantification of DAPI fluorescence showed that esg^{P3}/esg^{VS8} histoblast nuclei contained 7-16 times as much DNA as wild-type histoblast nuclei (Table 3). Assuming that wild-type histoblasts, arrested in G2 interphase, contain the 4C amount of DNA, esg^{P3}/esg^{VS8} histoblasts have 28-64C. This compares with approximately 85C for the larval epidermal cells of both OregonR and esg^{P3}/esg^{VS8}.

To determine whether *esg* mutant histoblasts are endoreplicating their DNA to become polyploid during larval stages, esg^{P3}/esg^{VS8} larvae were fed on food containing bromodeoxyuridine (BrdU) from 48 hours after egg laying. The incorporation of BrdU in the nuclei of third instar larvae was detected immunologically. Fig. 5A shows the epidermis from a control OrR wild-type larva. There is no apparent incorporation of BrdU in the nuclei of the histoblasts whereas adjacent larval epidermal cells show strong anti-BrdU staining. esg^{P3}/esg^{VS8} larvae showed overall less incorporation of the BrdU label but all nuclei in the vicinity of the landmark muscle insertion sites stained to the same extent with the anti-BrdU antibody indicating that these cells have replicated their DNA during larval development.

The abdominal phenotype of esg^{P3}/esg^{VS8} flies strongly suggests that the histoblasts fail to proliferate during metamorphosis. To examine the fate of histoblasts during metamorphosis the epidermis of wild-type and mutant pre-pupae and pupae was examined after staining with Hansen's Haematoxylin. In the wild type, at zero hours after puparium formation (APF), histoblasts are evident by their small size, relative to the larval cells, and their dense cytoplasmic staining (Fig. 6A). The position of the ventral histoblast nest can be determined by its proximity to three insertion sites for transverse muscles and a small larval cell (Madhavan and Schneiderman, 1977). This region of an esg^{P3}/esg^{VS8} pre-pupa at the same stage has no cells recognisable as histoblasts (Fig. 6B). The cells occupying the position of the ventral nest have a morphology similar to that of larval epidermal cells. At 24 hours APF wild-type histoblasts have proliferated and spread to replace most of the larval epidermal cells (Fig. 6C). A double row of larval cells remains along the segment boundary. In contrast, no proliferated histoblasts were observed in esg^{P3}/esg^{VS8} pupae (Fig. 6D). The epidermis of these animals consisted of larval cells which contained large lysosomes and many appeared to be degenerating. Proliferation of wild-type histoblasts is complete by 36 hours APF and differentiation of the adult abdomen has begun (Fig. 6E). Adult muscles have begun to form and cells that will give rise to the sensory organs are apparent. At this stage the abdomen of esg^{P3}/esg^{VS8} was composed of larval epidermal cells and no dorsal adult muscles were observed (Fig. 6F). It is apparent therefore that normal proliferation of histoblasts does not occur during metamorphosis of esg^{P3}/esg^{VS8} animals. This conclusion is supported by the failure of epidermis

Table 2. Quantification of abdominal histoblast number and size in *esg* mutant larvae

	Number of histoblasts			Size of nuclei (μm)	
genotype	aD	pD	V	$lacZ^+$	$lacZ^-$
$esg^{P3}/+$	14.5±2.4 (14)	6.0±0.9 (9)	12.9±1.6 (8)	6.3±1.0 (25)	12.3±1.4 (12)
esg^{P3}/esg^{VS8}	14.6±2.4 (16)	8.1±2.7 (14)	12.9±2.2 (22)	9.7±1.0 (18)	10.3±1.7 (12)
esg^{P3}/esg^{GW2}	14.8±2.0 (16)	8.5±0.8 (15)	12.7±2.4 (15)	9.8±1.4 (18)	10.5±1.7 (12)

Abdominal histoblasts of late third instar larvae were identified by X-gal staining of the esg^{P3} enhancer trap line. Histoblasts in A2-A7 nests were counted and their nuclear size determined. Averages and standard deviations are shown. The numbers of independent measurements are indicated in parentheses. aD, pD and V indicate anterior dorsal, posterior dorsal and ventral histoblast nests, respectively.

Table 3. Quantification of DAPI fluorescence in nuclei of wild-type and *esg* histoblasts and larval epidermal cells

Cell type	Relative fluorescence
OrR histoblast	32.8±6.9 (10)
esg^{P3}/esg^{VS8} histoblast	386.0±141.7 (10)
OrR larval cell	686.9±17.1 (11)
esg^{P3}/esg^{VS8} larval cell	680.0±19.7 (5)

Fluorescence is expressed in arbitrary machine units. Averages and standard deviations are shown. Numbers in parenthesis indicate the number of nuclei measured.

from 5 hour APF esg^{P3}/esg^{VS8} pre-pupae to incorporate BrdU during a 1 hour incubation in vitro whereas wild-type epidermis shows incorporation in proliferating histoblast nuclei when incubated under identical conditions (data not shown).

Phenotype of *raf esg* double mutant imaginal discs

Although *esg* expression is found in most of the imaginal discs, structures derived from *esg* mutant discs are relatively normal compared to the severe defects observed in *esg* mutant abdomens. One of the differences between imaginal discs and abdominal histoblasts is the temporal control of their cell division. During the larval period, imaginal disc cells actively divide while abdominal histoblasts are arrested in G2 interphase. To test the possibility that cell cycle arrest may sensitize imaginal disc cells to the effects of *esg* mutations, we examined the effect of *esg* mutations on imaginal discs mitotically arrested by a mutation in the *raf* gene. *raf* encodes a serine-threonine kinase essential for imaginal cell proliferation (Nishida et al., 1988). In animals lacking zygotic *raf* activity, imaginal disc cells fail to divide, which results in pupal lethality. Since most of the imaginal discs in *raf*- third instar larvae are very difficult to identify due to their small size, we chose to concentrate on the humeral disc because it is attached to the anterior spiracle and can be unambiguously identified. The identity of imaginal cells was confirmed by detecting expression of *lacZ* from the esg^{P3} enhancer trap element. Humeral discs in esg^{P3}/esg^{VS8} animals have nuclei similar in size to control discs (Fig. 7 A,B) and differentiate normal dorsal T1 structures (data not shown). The raf^{1} mutation greatly reduced the number of imaginal cells in the humeral disc while the size of their nuclei remained similar to the control (Fig. 7C). Combination of raf^{1} and esg^{P3}/esg^{VS8} greatly increased the size of the imaginal cell nuclei (Fig. 7D). In the most extreme case, the size of the mutant imaginal cell nuclei reached the size of the surrounding larval nuclei (Fig. 7F).

DISCUSSION

Phenotype of *esg* mutants

esg is expressed in a complex and dynamic striped pattern in the early embryo (Whiteley et al., 1992) and in the tracheal system (S. Hayashi, unpublished observations), but no clear relationship between these patterns of expression and mutant phenotype has been established. However, the expression pattern of *esg* in abdominal histoblasts and imaginal discs is, in general, consistent with the mutant phenotype observed in certain allelic combinations.

Most *esg* mutant alleles, including the apparent null esg^{L2} allele, are lethal at embryonic or early larval stages. However certain combinations of alleles allow survival to the adult or pharate adult stage. These flies show defects in imaginal structures, the most striking being a deletion, or partial deletion of the tergites and sternites. The abdominal cuticle is thin and transparent, reminiscent of the abdominal cuticle of flies that have had their histoblasts destroyed by X-irradiation as larvae (Roseland and Reinhardt, 1982). This suggests that the abdominal phenotype observed in these *esg* allelic combinations is due to a failure of histoblast proliferation. We have shown that *esg* mutant histoblasts do indeed fail to proliferate during metamorphosis leading to the observed phenotype.

Most of the viable mutant flies also showed a held-out wing phenotype and twisted legs are observed in certain allelic combinations. These defects are likely to reflect a requirement for the observed *esg* expression in the wing and leg imaginal discs. In addition, the reduced eye phenotype of rare esg^{P1}/esg^{GW21} pharate adults suggests that *esg* may be required in eye morphogenesis.

esg is required to maintain diploidy of histoblast cells

In situ hybridisation has shown that the *esg* gene is expressed in imaginal tissues late in embryogenesis and in third instar larvae. Additionally, *lacZ* expression from the esg^{P3} enhancer trap element is found in most imaginal tissues of the third instar larva. It is possible, therefore, that the role of the *esg* gene product is to regulate genes that determine tissues as being imaginal as opposed to larval, or that maintain the imaginal state. Since abdominal histoblasts and imaginal discs are apparent in $esg^{P3}/Df(2L)A48$ embryos, a role for *esg* in specifying these tissues seems unlikely. Although a primary specifying role for *esg* cannot be ruled out it is perhaps more likely that *esg* is responsible for maintaining the imaginal state.

We have shown that *esg* mutations cause an increase in histoblast nuclear size, increased *lacZ* expression from the esg^{P3} enhancer trap element and increased PID and DAPI staining. The simplest interpretation of these results is that the normally diploid histoblasts have become polyploid by endoreplicating their DNA during larval development. This theory is supported by the incorporation of BrdU into the nuclei of cells occupying the position of the anterior dorsal histoblast nest during larval development. One of the functions of *esg* may therefore be to maintain diploidy in histoblast cells, thus allowing them to enter the mitotic cycle during metamorphosis.

esg function in imaginal discs

This proposed role for *esg* must be reconciled with the observed defects in structures derived from the imaginal discs. While the abdominal defects are essentially due to deletion of histoblast-derived structures, the leg and wing defects are limited to malformation. This difference in sensitivity to *esg* mutations may reflect the different temporal

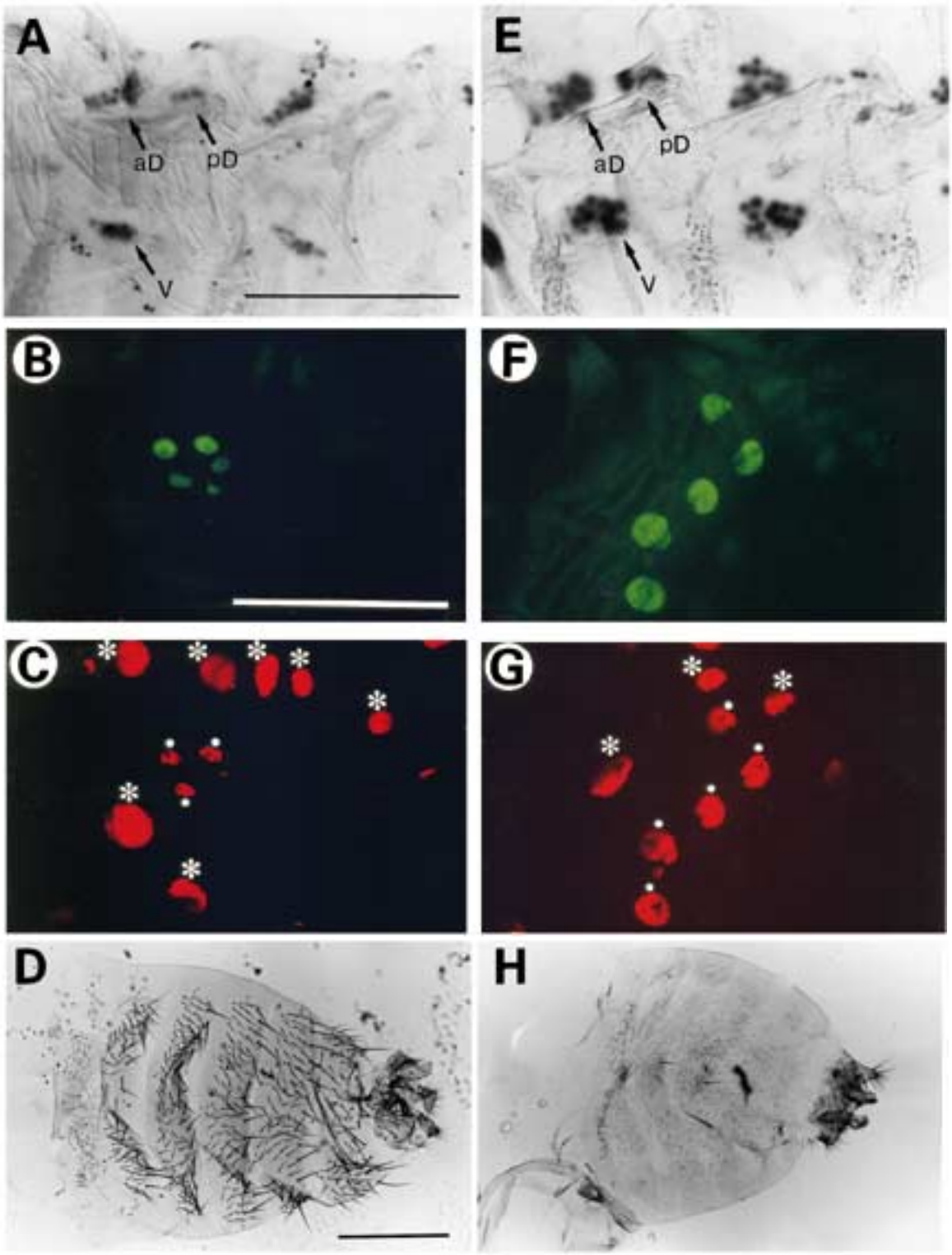

Fig. 4. Phenotype of *esg* mutant histoblasts. *lacZ* expression, PID staining and cuticle pattern of esg^{P3}/+ (A-D) and esg^{P3}/esg^{VS8} (E-H) animals are compared. esg^{P3}/+ animals develop normally and serve as a control. (A,E) X-gal staining pattern of epidermis from third instar larvae. aD, pD and V indicate anterior dorsal, posterior dorsal and ventral histoblast nests respectively. (B,F) *lacZ* expression in histoblasts visualized by anti-β-galactosidase immunofluorescence staining visualized by confocal microscopy. (C,G) PID staining pattern of the same fields as above. Small asterisks indicate histoblast nuclei and large asterisks indicate epidermal cell nuclei.
(D,H) Abdomens of pharate adult males of each genotype. In H, almost all of the tergites (and sternites, not shown) of A2-A6 are deleted. Scale bars in A and D, 5005 μm; in B, 505 μm.

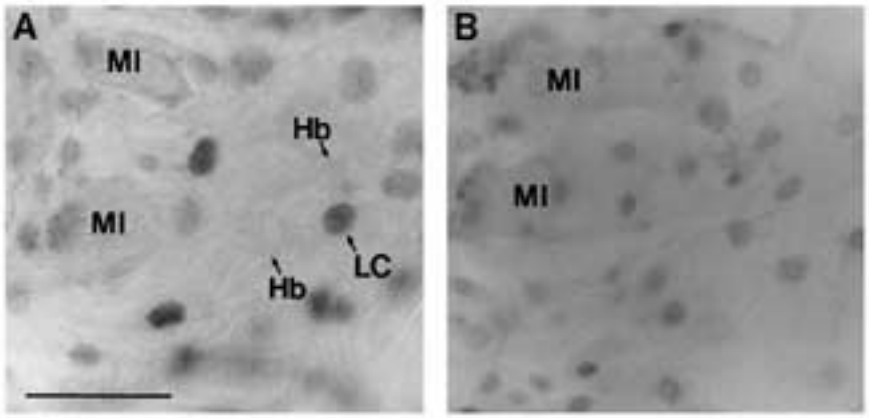

Fig. 5. BrdU incorporation into nuclei of epidermal cells during larval development. Larvae were fed on BrdU-containing food from 48 hours after egg laying and dissected at the wandering third instar stage. (A) OrR wild-type anterior dorsal histoblast nest and surrounding epidermis. No incorporation is detectable in the histoblast nuclei. The nuclei of the larval epidermal cells have been labelled strongly. (B) The same region as A of a esg^{P3}/esg^{VS8} larva. All nuclei have been labelled to the same extent. MI, muscle insertion site; Hb, histoblast nucleus; LC, larval epidermal cell nucleus. Scale bar (for A and B), 100 μm.

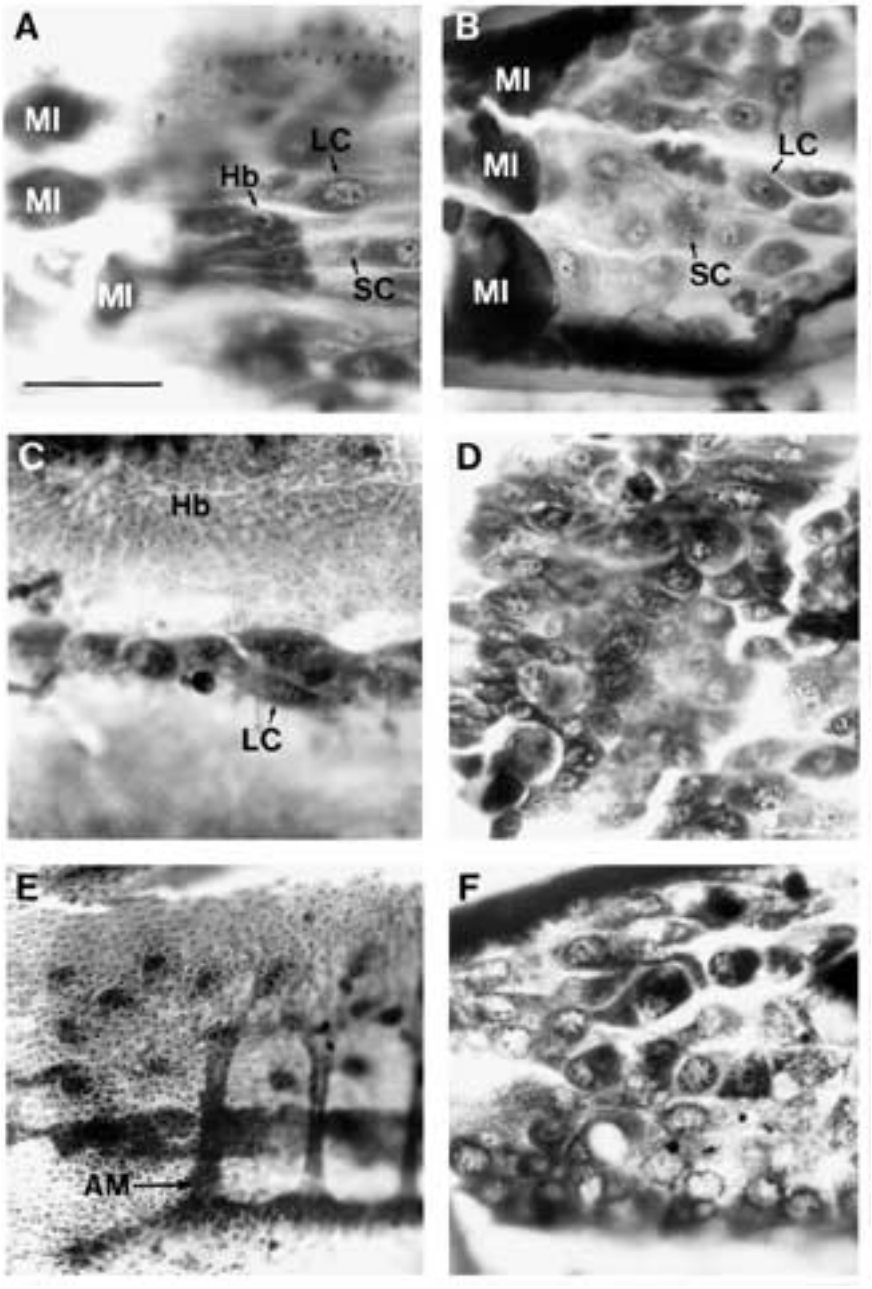

Fig. 6. The phenotype of OrR wild-type (A,C,F) and esg^{P3}/esg^{VS8} (B,D,F) epidermis during metamorphosis. Puparia were dissected, fixed and stained with Hansen's Haematoxylin at 0 (A,B), 24 (C,D) and 36 (E,F) hours after puparium formation. (A,B) Ventral histoblast nest and surrounding epidermis. In A, histoblasts are apparent by their small size and densely staining cytoplasm. In B, all cells have a morphology similar to that of the larval epidermal cells. MI, muscle insertion site; Hb, histoblast; SC, small cell; LC, larval epidermal cell. (C,D) Dorsal view of the epidermis at the segmental boundary. In C, the histoblasts have proliferated and spread to replace most of the larval epidermal cells. A double row of epidermal cells remains at the segment boundary. In D, no histoblast cells can be seen. The larval cells have become disorganised and a proportion of them appear to be degenerating. (E,F) Dorsal view of the epidermis at the segmental boundary. In E replacement of epidermal cells is complete and adult muscles have begun to form. In F the epidermis still consists of larval cells. There are no adult muscles. AM, adult muscle. Scale bar in A, 100 μm. All photographs are at the same magnification.

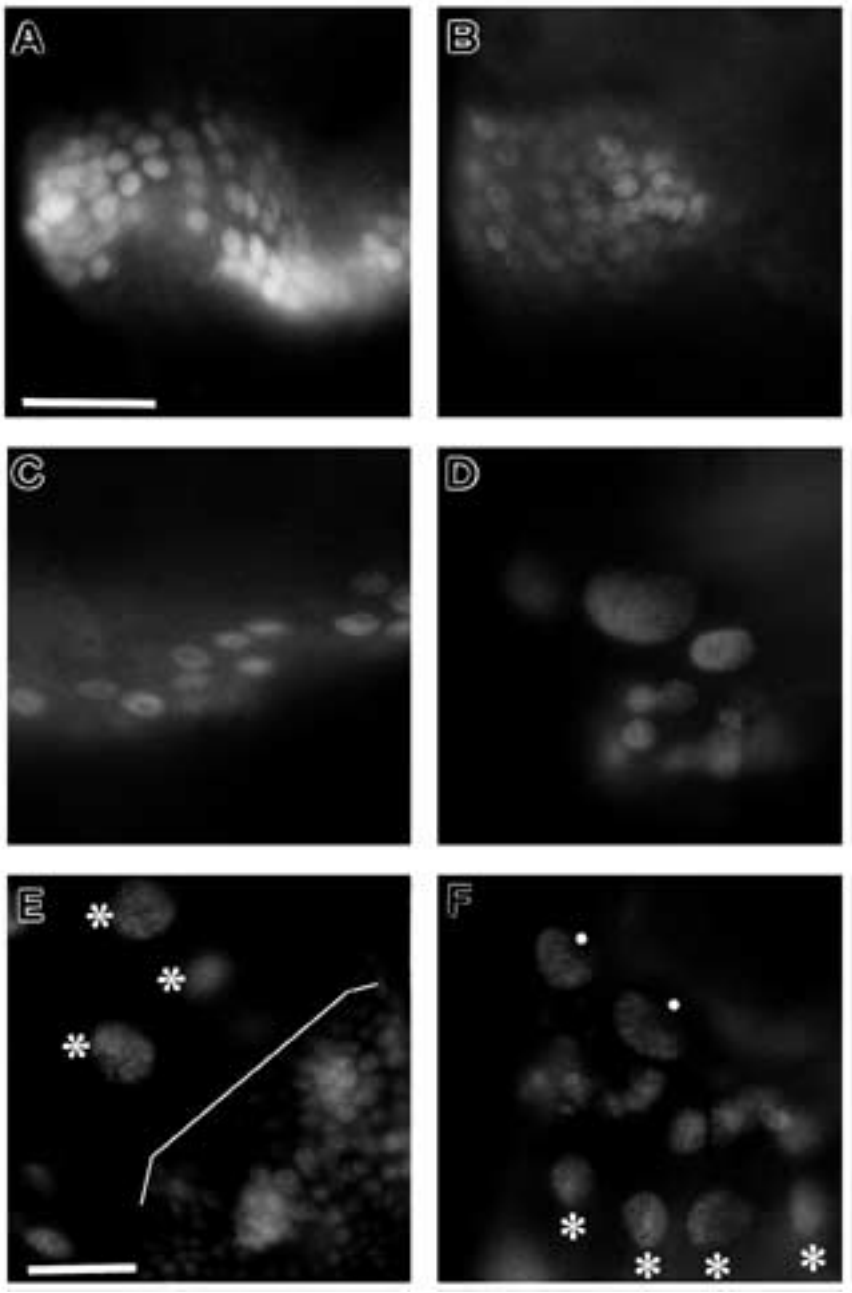

Fig. 7. Phenotype of *raf*^{1};*esg*^{P3}/*esg*^{VS8} humeral discs. (A-D) Anti-β-galactosidase immunofluorescence staining of humeral imaginal discs which are attached to anterior spiracles. The staining reveals imaginal cells expressing the *lacZ* gene from the *esg*^{P3} enhancer trap element. Genotypes are: A, *esg*^{P3}/+; B, *esg*^{P3}/*esg*^{VS8} ; C, *raf*^{1} and D, *raf*^{1};*esg*^{P3}/*esg*^{VS8}. (E,F) PID staining of *esg*^{P3}/+ (E) and *raf*^{1};*esg*^{P3}/*esg*^{VS8} (F) humeral discs. In E, note the difference in size between the imaginal cell nuclei (marked with a bracket) and the larval cell nuclei of the anterior spiracle (large asterisks). In F, imaginal cells identified by expression of the *lacZ* gene (small asterisks) are large and are indistinguishable in size from the larval cells (large asterisks).

pattern of cell division in imaginal discs and abdominal histoblasts. While imaginal disc cells are actively dividing during larval stages, abdominal histoblasts are arrested in G2 interphase. The histoblasts enter mitosis only after pupariation under the influence of a change in hormonal environment. Cell cycle arrest of the abdominal histoblasts during larval stages, in addition to a reduction in *esg* activity, may be the necessary condition to become polyploid. This explanation is supported by the phenotype of *esg* humeral imaginal disc cells which have additionally been mitotically arrested by a mutation in the *raf* gene. This resulted in a marked increase in nuclear size. It thus appears that ploidy of imaginal disc cells may also be increased by mutations in the *esg* gene but that *esg* function is not required to maintain diploidy as long as they continue to divide.

esg may have an additional function in imaginal discs. The correlation of localised *esg* expression in imaginal discs and defects in adult structures of *esg* mutants suggests that spatially restricted *esg* expression is required for some aspects of imaginal disc development even when they are competent to divide. To investigate further the function of *esg* in imaginal discs, mosaic analysis of strong *esg* alleles will be necessary.

It is not clear at present what significance the proposed role of the *esg* gene in maintenance of ploidy has for the late embryonic or early larval lethality of the presumed null alleles such as *esg*^{L2}. If *esg* function is required only in imaginal tissues, null alleles may be expected to cause pupal lethality. The earlier patterns of *esg* expression may therefore be required for survival beyond the first larval instar. However, it is unknown whether *esg* functions to regulate ploidy levels at these stages.

We thank Michael Ashburner, John Roote, Allen Spradling, Chris Doe, Yasuyosi Nishida and Matt Scott for stocks, Yuh-Nun Jan, John Tamkun and Matt Scott for *Drosophila* cDNA and genomic libraries and Martin McAinsh for his assistance in quantifying DAPI fluorescence. Matt Scott generously allowed the authors to study the esg^{P2} line, which was isolated in his laboratory. S. Hayashi and S. Hirose owe much to Takao Watanabe (Genetic Stock Center, National Institute of Genetics) for his help in starting a *Drosophila* project in their lab. This work has been supported in part by Grants-in-Aid for Scientific Research from the Japanese Ministry of Education, Science and Culture to S. Hayashi and to S. Hirose and by grants from the UK Royal Society and the Science and Engineering Research Council to A. D. S.

REFERENCES

Ashburner, M., Thompson, P., Roote J., Lasko, P. F., Grau, Y., El Messal, M., Roth, S. and Simpson, P. (1990). The genetics of a small autosomal region of *Drosophila melanogaster* containing the structural gene for alcohol dehydrogenase. VII. Characterization of the region around the *snail* and the *cactus* loci. *Genetics* **126**, 679-694.

Ashburner, M. (1989). *Drosophila*: *A Laboratory Manual*. Cold Spring Harbor, New York: Cold Spring Harbor Laboratory Press.

Bier, E., Vaessin, H., Shepherd, S., Lee, K., McCall, K., Barbel, S., Ackerman, L., Carretto, R., Uemara, T., Grell, E., Jan, L. Y., and Jan, Y. N. (1989). Searching for pattern and mutation in the *Drosophila* genome with a P-lacZ vector. *Genes Dev.* **3**, 1273-1287.

Bryant, P. J. (1978). Pattern formation in imaginal discs. In *The Genetics and Biology of* Drosophila (eds. M. Ashburner and T. R. F. Wright), 2c: pp. 230-335. London: Academic Press.

Ephrussi, A., Dickinson, L. and Lehman, R. (1991). oskar organizes the germ plasm and directs localization of the posterior determinant nanos. *Cell* **66**, 37-50.

Kramer, H. and Zipursky, L. (1990). Whole mount in situ hybridization to imaginal discs using digoxigenin labeled DNA probes. In *Drosophila Information Newsletter* **1**, (Eds. C.Thummel and K. Matthews).

Lindsley, D. L. and Zimm, G. G. (1992). *The Genome of* Drosophila melanogaster. San Diego: Academic Press Inc.

Madhavan, M. M. and Schneiderman, H. A. (1977). Histological analysis of the dynamics of growth of imaginal discs and histoblast nests during the larval development of *Drosophila melanogaster*. *Roux's Arch. Dev. Biol*. **183**, 269-305.

Nishida, Y. Hata, M., Ayaki, T., Ryo, H., Yamagata, M., Shimizu, K. and Nishizuka, Y. (1988). Proliferation of both somatic and germ cells is affected in the *Drosophila* mutant of the *raf* proto-oncogene. *EMBO J*. **7**, 775-781.

Pearson, M. J. (1974). The abdominal epidermis of *Calliphora erythrocephala* (Diptera). I Polyteny and growth in the laval cells. *J. Cell Sci.* **16**, 113-131.

Robertson, H. M., Preston, C. R., Phillis, R. W., Johnson-Schlitz, D. M., Benz, W. K. and Engels, W. R. (1988). A stable source of P element transposase in *Drosophila melanogaster*. *Genetics* **118**, 461-470.

Roseland, C. R. and Scheneiderman, H. A. (1979). Regulation and metamorphosis of the abdominal histoblasts of *Drosophila melanogaster*. *Roux's Arch. Dev. Biol*. **186**, 235-265.

Roseland, C. R. and Reinhardt, C. (1982). Abdominal development. In *A Handbook of* Drosophila *Development* (ed. R. Ransom), pp. 215-235. Amsterdam: Elsevier.

Solcia, E. (1973). In *The Encyclopaedia of Microscopy and Microtechnique* (ed. P. Gray), pp. 238-248. New York: Van Nostrand Reinhold Co.

Tautz, D. and Pfeifle, C. (1989). A non-radioactive in situ hybridization method for the localization of specific RNAs in *Drosophila* embryos reveals translational control of the segmentation gene *hunchback*. *Chromosoma* **98**, 81-85.

Tomlinson, A. and Ready, D. F. (1987). Neuronal differentiation in the *Drosophila* ommatidium. *Dev. Biol*. **120**, 366-376.

Whiteley, M., Noguchi, P. D., Sensabaugh, S. M., Odenwald, W. F. and Kassis, J. A. (1992). The *Drosophila* gene *escargot* encodes a zinc finger motif found in *snail*-related genes. *Mech. Dev*. **36**, 117-127.

(Accepted 15 February 1993)